The role of LKB1 in melanoma metastasis and PD-L1 expression

Undergraduate Research Thesis

Presented in partial fulfillment of the requirements for graduation *with honors research distinction* in the undergraduate colleges of The Ohio State University.

by

Reena Meghan Underiner

The Ohio State University
April 15, 2016

Project Advisor: Dr. Christin E. Burd, Department of Molecular Genetics

Abstract

For melanoma patients with metastatic, NRAS-mutant tumors, treatment options are limited. However, the recent FDA approval of immune checkpoint inhibitors (e.g. PD-1 and PD-L1 inhibitors) has brought new hope these patients. While responses to these drugs are often durable and robust, only a subset of melanoma patients will benefit from therapy. Morevoer, biomarkers to accurately predict which patients will respond are desperately needed. Recent studies have linked loss of the Liver Kinase B1 (*LKB1*) tumor suppressor gene to melanoma metastasis, as well as suggested a potential relationship between LKB1 and PD-L1 expression. Thus, LKB1 may be useful as a biomarker for predicting patient response to immune checkpoint inhibitors. Here, we created NRAS-mutant melanoma cell lines with differing *LKB1* status to evaluate the role of this protein in migration. We find that restoration of LKB1 inhibits cellular migration. Using genetically engineered mouse models, we confirm this finding by showing that the loss of *Lkb1*, in combination with *NRAS*-mutation and ultraviolet (UV) light exposure, promotes metastatic melanoma progression. Finally, we discovered that restoration of kinase-deficient or proficient LKB1 activity in several melanoma cell lines leads to increases in PD-L1 expression. Together these data provide evidence that *LKB1* loss may be a marker of metastatic progression and of resistance to immune checkpoint inhibitor therapies.

Keywords: melanoma, metastasis, LKB1, PD-L1, checkpoint inhibitor therapy

Introduction

In 2016, the American Cancer Society predicts that 76,380 new melanomas will be diagnosed and 10,130 people will succumb to the disease [1]. *In situ* and early-stage melanomas are curable; however, metastatic melanoma is one of the deadliest cancer types, with a 5-year survival rate of only 17%[1]. Although the incidence of metastatic melanoma has steadily increased over recent decades, it can be expected to rise even further in upcoming years due to the aging U.S. population. For a long time, treatment options for metastatic melanoma patients were limited, and due to the rapidity in which melanomas metastasize, surgical excision was rarely curative. In fact, as of 2011, the US Food and Drug Administration had approved only two drugs for the treatment of advanced metastatic melanoma: decarbazine, a chemotherapy which

was approved in 1975, and high-dose interleukin-2 (IL-2), an immunological therapy which was approved in 1998[2] [2]. These drugs showed limited success in patients, with decarbazine shrinking tumors 12.5% of the time[3] and IL-2 being curative in only 4% of patients[4]. Furthermore, response to these drugs was often limited, as many tumors grew resistant[5].

Fortunately, in the last five years, multiple efficacious drugs were approved for the treatment of melanoma. These new therapies can be divided into two categories: BRAF inhibitors and immune checkpoint inhibitors. BRAF, which is mutated in approximately 50% of melanoma patients, is a kinase which activates the downstream ERK pathway through phosphorylation of MEK, thereby promoting cell proliferation and survival. BRAF-mutant inhibitor therapies, such as vemurafenib and dabrafenib, have high response rates in melanoma patients and improve patient survival [6]. However, limitations remain. For example, treatment durability is a problem, as tumor cells rapidly develop resistance to BRAF inhibitors[6]. Additionally, though *BRAF* mutations are found in many melanoma patients, approximately one third of patients harbor mutually exclusive mutations in the proto-oncogene, *NRAS*. These patients do not respond to BRAF inhibitor therapies. Checkpoint inhibitor therapies target the immune system, leading to enhanced tumor cell recognition and elimination. In the human body, all cells contain MHC Class I proteins that display antigens on the surface of the cell for recognition by the immune system. Cancer cells, however, produce many mutated proteins, and therefore may display abnormal antigens, called neoantigens, on the surface of the cell. These neoantigens enable T-cells to recognize the tumor cell as foreign and initiate a response against them. Tumor cells, however, have found a way to evade immune recognition, through complex interactions between the Programmed Death 1 (PD-1) receptor on T cells and Programmed Death Ligand 1 (PD-L1)

on tumor cells (Fig. 1A). Checkpoint inhibitor therapies, such as pembrolizumab and nivolumab (PD-1 inhibitors), successfully in block the PD-L1-PD-1 interaction, thereby allowing the immune system to once again respond to neoantigens expressed on the tumor cell surface (Fig. 1B) [7]. Unlike chemotherapies and BRAF inhibitors, responses to immune checkpoint therapies appear more durable. However, it is unknown why some patients respond to immunotherapy while others do not. Only a small subset of melanoma patients (up to 40%) respond to approved checkpoint inhibitor therapies (ie. tumor regression or stabilization of disease), yet more than half of these individuals achieve long-term responses lasting more than one year[8]. Since these therapies can be toxic and costly, robust biomarkers are desperately needed to predict the approximately 40% of patients that will respond. There are currently no targeted agents approved to treat NRAS-mutant tumors, which are notoriously aggressive. To increase the cure rate of these patients, two options should be considered: prevent metastasis or improve responses to immune checkpoint inhibitor therapies, such PD-L1 inhibitors.

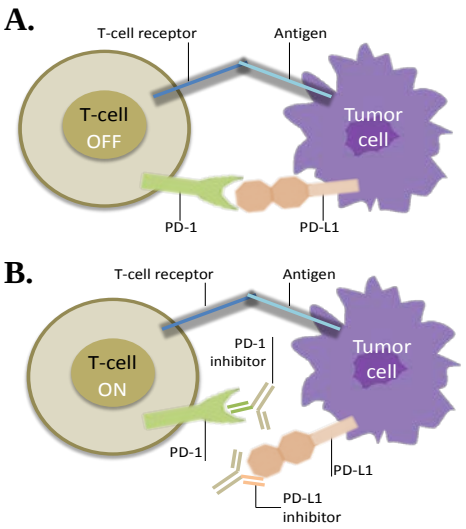

Figure 1, **Tumor cells evade the immune system through PD-L1 expression. A**, Diagram illustrating a mechanism of immune system evasion in tumor cells. Tumor cells bind to T-cells and deactivate them via PD-1-PD-L1 interaction. **B**, Diagram demonstrating the mechanism by which checkpoint inhibitor therapies can promote normal immune response to tumor cells. These immunotherapy drugs bind to the PD-1 receptor or PD-L1 ligand, inhibiting the tumor cells from deactivating the T-cells. *Image loosely based on figure by Guha et al, (2014).*

Several studies show that mutations in the Liver Kinase B1 (*LKB1*) tumor suppressor gene are linked to metastatic potential in lung adenocarcinomas[9], breast cancers[10], and melanoma[11]. A more recent study also demonstrates that the loss of LKB1 expression

promotes metastasis in a $KRAS^{G12D}$-driven murine melanomas[12]. However, as *NRAS* mutations vastly outweigh the number of *KRAS* mutations in human melanoma, the clinical relevance of that study is unclear. In comparison to *KRAS* mutations, which are present in roughly 2% of human melanomas, NRAS-driven tumors are far more representative, occurring in up to 30% of lesions[13]. Consequently, a portion of the present study focused on elucidating the role of LKB1 and its kinase activity in the metastasis of NRAS-driven melanoma, through both *in vitro* and *in vivo* models. As several lung cancer studies have also noted a correlation between *LKB1* loss and elevated PD-L1 expression[14, 15], the present study also explored the relationship between LKB1 kinase function and PD-L1 expression in melanoma.

Materials and Methods

Generation of melanoma cell lines with differing LKB1 status

In several *LKB1*-null murine melanoma cell lines (NL212, NL216, and NL145) as well as a human melanoma cell line (SK-MEL 103), LKB1 was reintroduced, either in a fully functional form (LKB1) or a kinase-dead version (LKB1-KD). LKB1 infection was also performed on one LKB1-proficient human melanoma cell line (SK-MEL 147. LKB1 and LKB1-KD lentivirus was generated via polyethylenimine (PEI) transfection of 293T cells with either pBABE FLAG-LKB1 or FLAG LKB1-KD plasmids (2 μg), as well as the pCMV-VSV-G envelope (0.222 μg) and pUMVC packaging plasmids (1.176 μg). 16 μL of PEI transfection reagent (1 mg/mL) was added to the plasmids and then pipetted onto the host cells. Cells were incubated for 1 hour in serum-free media, after which full media was returned and changed the following day (day 2). On day 3, virus was collected from the transfected cells, the media was filtered to eliminate any 293T cells, and frozen for future use.

Target cell lines were infected with 5 mL of viral media and 5 mL of growth media, along with 10 μL of polybrene (10 mg/mL). Infection was repeated on day two to further increase transduction efficiency. Media was changed following each infection and cells were allowed to recover for two days, after which puromycin was added (according to drug optimization curves: 30 μg/mL for murine lines, 10 μg/mL for human lines) to begin selection. Cells underwent selection for 5-7 days.

Immunoblot Analysis for LKB1 Detection

Immunoblots were performed on protein samples from all generated cell lines to confirm the expression of LKB1. Cells were lysed using RIPA buffer and PMSF protease inhibitors (1:100), then sonicated. Protein concentration was measured via Bradford Assay. All blots were run on 10% SDS-Page gels and transferred to 0.45 μm nitrocellulose membranes. Membranes were blocked in a solution of 1% cold water fish gelatin in phosphate-buffered saline, and incubated in anti-LKB1 antibody (1:1000; Cell Signaling Technology, Cat. #3050) overnight. After washing 3x with Tris-buffered saline with 0.1% Tween-20 (Sigma), membranes were incubated in anti-rabbit fluorescent secondary antibody (IRDye 800CW 1:20,000; Licor Cat.# 926-32211) for 45 minutes. To control for variations in the amount of protein loaded, membranes were also blotted for β-actin (1:2500; Cell Signaling Technology, Cat. #4967). Membranes were imaged using the Li-Cor Odyssey CLx Imaging System and analyses were performed using Image Studio software.

Migration Assays

Migration assays (Figure 3A) were performed in the murine cell lines. First, 12-well plates were coated in collagen for 3 hours after which cells were seeded and grown to confluency. To eliminate the effects of cell proliferation and ensure only migration was being assessed, the cells were treated with mitomycin C for 8 hours (according to drug optimization curves: 5 μg/mL for the NL212 and NL216 lines, 1.5 μg/mL for the NL145 line). After the 8-hour mitomycin C treatment, a 1 mm scratch was created in a straight, vertical line across the dish using a 1000 μL sterile pipet tip. Media was changed to remove any floating cell debris, and a photograph was taken of the initial scratch at t=0h. Cells were permitted to migrate for 18 hours, after which another photograph was taken at t=18h. Using ImageJ software, the percentage of wound closure was determined. All migration assays were performed in biological triplicates to verify results. Statistical significance was determined by 1-way ANOVA analysis.

PD-L1 flow cytometry

LKB1-null, LKB1 re-expressing (WT), and LKB1-KD cell lines were individually seeded to reach a density of 50-60% in 20 hours. They were then lightly trypsinized, centrifuged for 3 minutes at 1200 RPM to remove any dead cells, and counted using a Coulter Counter. Approximately 500,000 cells were aliquotted per tube and tubes were kept on ice throughout the remaining steps. Cells were centrifuged once more (3 minutes, 1200 RPM) and resuspended in fluorescence-activated cell sorting (FACS) buffer (5% BSA in PBS). PE-conjugated PD-L1 antibody (Biolegend, Cat.# 124308) and PE-conjugated Isotype Control antibody (Biolegend, Cat.# 400636) were added to their respective tubes at a 1:100 concentration, and allowed to incubate for 45 minutes in the dark at 4°C. Cells were then washed three times with FACS

buffer, resuspended in cold PBS, and filtered through a 40 μm cell strainer to remove any cell clumps. Cells were then immediately analyzed using a FlowSight Flow Cytometer (EMD Millipore, Model # 100300). The PE fluorophore was measured using the 488 nm excitation laser, set to 560-595 nm (channel #3). Results were quantified using IDEAS software (EMD Millipore), with gates set so that isotype controls had ≤1% of cells marked positive.

Murine Alleles and Husbandry

Genetically engineered mouse models containing conditional knock-in (i.e. *LSL-N-Ras*^{Q61R}[16, 17] and *Rosa26-YFP*[18]) and knock-out (i.e. *p16*^{L}[19] and *LKB1*^{L}[12]) alleles (Herein, referred to as *TpLNR* mice), were used to evaluate the relationship between UV exposure, *Lkb1* loss, metastasis, and PD-L1 expression. *TpLNR* mice were compared to *TpNR* mice, which contain the same *LSL-N-Ras*^{Q61R}, *Rosa26-YFP*, and *p16*^{L} conditional alleles but have a functional *Lkb1* allele. *Tyrosinase- CRE ER*^{T2} was used to drive the expression of a 4OHT-inducible CRE recombinase specifically in melanocytes. As shown in Figure 5A, in the conditional *p16*^{L} allele, CRE recombination causes the excision of exon 1 α, preventing the expression of *p16*^{INK4a} but maintaining *p19*^{ARF}. In the conditional *LKB1*^{L} knock-out allele, CRE recombination results in the excision of exons 3-6. The *LSL-N-ras*^{Q61R} and *Rosa26-YFP* alleles are knock-ins that conditionally expresses N-RAS^{Q61R} and YFP, respectively, upon removal of a transcriptional stop element (3xSTOP) by CRE-mediated recombination. Green arrowheads denote the location of loxP recognition sites, which are excised during CRE-medicated recombination. All animal work was conducted in accordance with protocols approved by the Institutional Animal Care and Use Committee (IACUC) at the Ohio State University (IACUC protocol #2012A00000134).

Induction of CRE Recombinase via 4-OHT and UVB treatment

To characterize the organs to which melanomas metastasize in mice lacking *Lkb1* and further study the relationship between LKB1 and PD-L1, tumors were induced in four litters of *TpLN*^{Q61R} mice. On postnatal days 1 and 2, pups were painted with 4-hydroxytamoxifen (25 mg/mL) dissolved in dimethyl sulfoxide to stimulate CRE-ERT2 activity, leading to expression of NRAS^{Q61R} and loss of *p16* and *LKB1*. On day 3, mice were split into ultra-violet (UV) exposure and non-exposure groups at a 3:1 ratio. Mice in the UV exposure group were exposed to 4.5 kJ/m^2 UV radiation to evaluate the effect of UV radiation on metastasis in NRAS-driven, *LKB1*-deficient melanomas.

Assessment of melanomas

Each cohort of mice was checked twice weekly for the formation of new tumors. Once a new tumor was noted, tumor growth was assessed at least 5 times per week by digital caliper measurements of the tumor dimensions [width x length (mm)] until IACUC exclusion criteria for tumor burden or comorbidities were met. Necropsies were then performed and primary tumor and organs with potential macrometastases (commonly the tumor proximal lymph nodes and the spleen) were harvested. After formalin fixation and paraffin embedding, these tissues were evaluated for histological abnormalities, and stained for PD-L1. For analysis purposes, tumor growth was normalized to day 1 and linear regression models of tumor growth created using GraphPad Prism software. Analysis of melanoma-free survival, overall survival, tumor burden, and tumor growth rates were also performed with GraphPad Prism software. Gehan-Breslow-Wilcoxon tests were performed for each experimental group to assess the statistical significance

of tumor-free survival; Mann-Whitney tests were used to determine the statistical significance of average tumor burden and linear regression of tumor growth between the groups.

Results

Generation of stable *LKB1* and *LKB1-KD* cell lines via lentiviral transduction

The loss of *Lkb1* has been implicated in enhanced metastasis in *KRAS*-driven melanomas [12]; however, the role of this protein and its kinase activity has never been addressed in *NRAS*-mutant melanomas. In order to address the role of this protein in melanocytic migration, melanomagenesis, and PD-L1 expression, melanoma cell lines were created with varying LKB1 status. Immunoblot of human melanoma cell lines revealed that SK-MEL 103 cells are LKB1-deficient (Figure 2A). By contrast, SKMEL-147 cells are LKB1-proficient. Previous assays performed in our lab have also confirmed that both lines are heterozygous for a $NRAS^{Q61R}$ mutation. In addition to these human melanoma cell lines,the murine lines NL212, NL216, and NL145, which were developed from tumors of *TpLN* mice (*NRas*-mutant, *p16*-deficient and *Lkb1*-deficient), were also chosen to

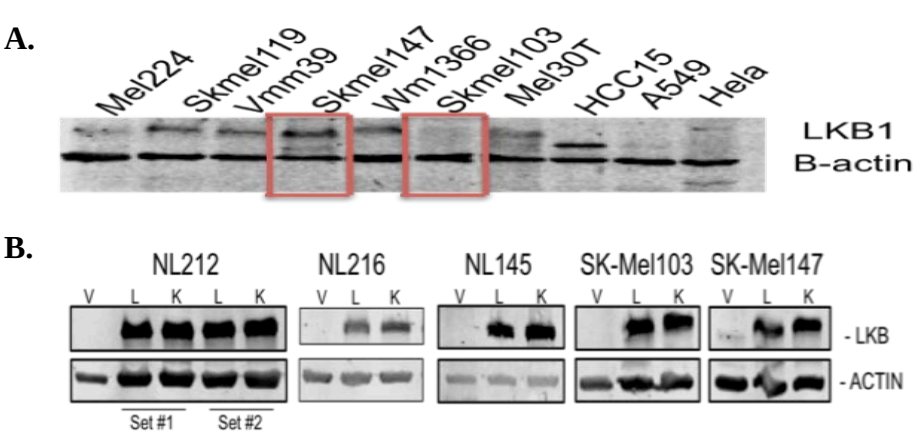

Figure 2. Establishment of melanoma cell lines with differing LKB1 status. A, Immunoblot of LKB1 in human melanoma cell lines. The SK-MEL 103 cell line is LKB1-deficient, whereas the SK-MEL 147 line is LKB1-proficient. **B**, Immunoblot demonstrating the successful integration of lentiviruses encoding LKB1 and LKB1-KD (kinase dead) in three murine (NL212, NL216, NL145) and two human cell lines (SK-MEL 103 and SK-MEL 147). Here, V = vehicle (*Lkb1*-null), L = LKB1-proficient, and K = LKB1 kinase-dead. Two distinct clones of NL212 were generated by separate lentiviral transductions, distinguished by Set #1 and Set #2.

study the role of LKB1. Infection and puromycin selection of NL212, NL216, NL145, SK-MEL 103, and SK-MEL 147 cell lines with lentiviruses encoding either LKB1 or LKB1-KD resulted in the generation of stable cell lines (Figure 2B).

Restoration of *LKB1* inhibits cellular migration

Migration assays were performed in NL212, NL216, and NL145 cells to evaluate the impact of LKB1 status on migratory potential (Figure 3A). As we hypothesized that the LKB1 tumor suppressor was important in preventing metastasis, we expected to see that cell lines with functional *Lkb1* would experience reduced migration, whereas cell lines with loss of *Lkb1* would experience enhanced migration. Consistent with

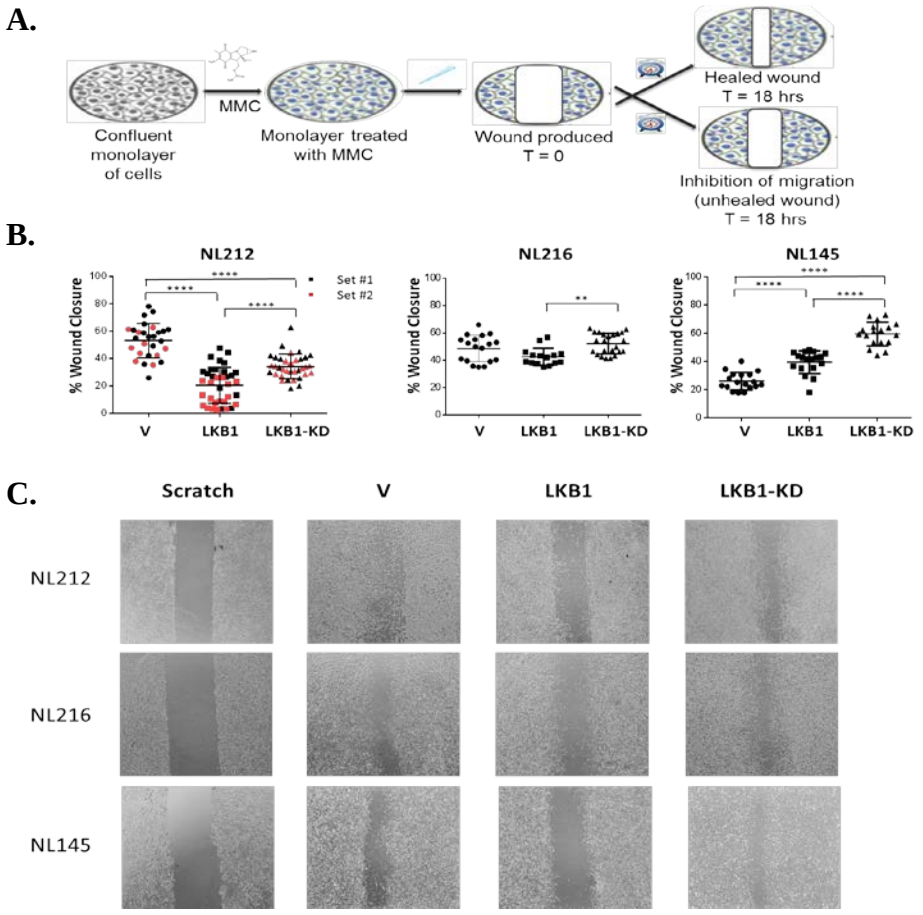

Figure 3. Restoration of LKB1 inhibits cellular migration. A, Diagram illustrating the protocol followed for wound healing assays. MMC represents mitomycin C treatment, employed to prevent cell proliferation during the assay. **B**, Area of wound and percent wound closure in three cell lines, NL212, NL216, and NL145, was measured using ImageJ software. Here, V = vehicle (*Lkb1*-null), LKB1 = LKB1-proficinet, and LKB1-KD = LKB1 kinase-dead. Two distinct clones of NL212 were produced by separate lentiviral transductions, distinguished by Set #1 and Set #2. Significance values are denoted by asterisks, with ** indicating P ≤ 0.01 and **** indicating P ≤ 0.0001. All wound healing assays were performed in triplicate. **C**, Representative images of wound healing assays at T = 0 and T =18 for LKB1-deficient and –proficient cell lines.

our hypothesis, results demonstrated that the introduction of LKB1 into the NL cells lines limits their migration (33.31% reduction in migration in NL212, 6.13% in NL216) (Figure 3B-C). A reduction in migration was not seen in the NL145 cell line. This could be partially explained by the *Lkb1*-null line's intolerance to mitomycin C treatment, which may have influenced the migratory rate. In the NL212 cell line, introduction of LKB1-KD resulted in a partial limitation in migration (18.77%), though not as completely as when introduced with LKB1 (33.31%). Though consistent with the NL212 results, the NL216 results were much less dramatic; restoration of LKB1insignificantly limited migration (6.13%) and LKB1-KD migratory rates matched those of the LKB1-null. In the NL145 cell line, introduction of LKB1-KD dramatically increased migration (33.44%). Though variable among the NL cell lines, migration rates in LKB1-KD cell lines reveal that LKB1 kinase activity may be important, but not solely responsible for the reduction in cell motility.

Restoration of kinase-deficient and –proficient LKB1 increases PD-L1 expression

Several studies have implicated a potential relationship between *LKB1* status and PD-L1 expression in lung cancer, though one has yet to be established in melanoma. Should a relationship between *LKB1* status and PD-L1 expression exist in melanoma, it is possible that *LKB1* may be able to be used as a biomarker for response to immune checkpoint inhibitor therapies, such as PD-L1 inhibitors. For instance, if it is found that LKB1 regulates PD-L1, then it is possible that *LKB1*-null tumors would not respond to a PD-L1 inhibitor, as the inhibitor would not have a target. To investigate the potential for *LKB1* as a biomarker for checkpoint inhibitor therapies, flow cytometry was employed to evaluate PD-L1 expression in murine melanoma cell lines with differing LKB1 status. Across all lines, *LKB1*-null cells had low PD-

L1 expression (<22%). With restoration of LKB1, PD-L1 expression increased in two of the three cell lines, though the amount varied by line (Figures 4A-B). The NL212 line showed the most significant change, with an average increase in PD-L1 expression of 57.7% when LKB1

A.

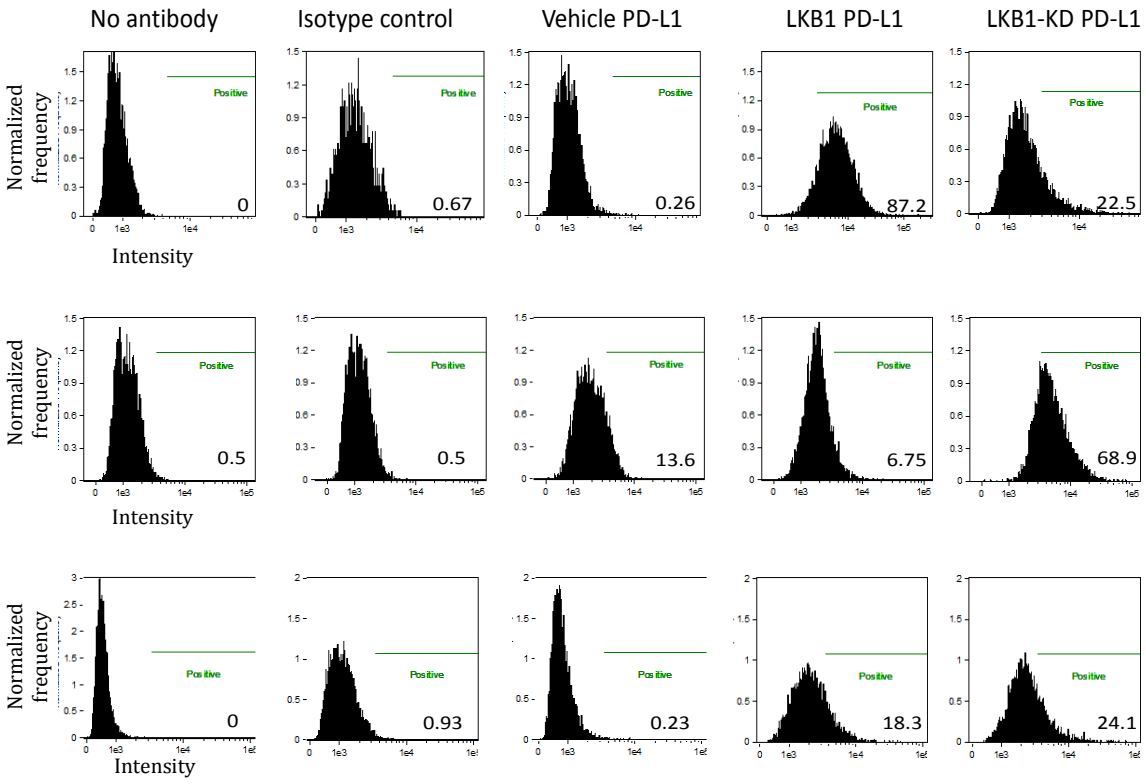

B.

	No antibody	Isotype Control	Vehicle PD-L1	LKB1 PD-L1	LKB1-KD PD-L1
NL212	0.20 ± 0.39	0.59 ± 0.60	3.56 ± 6.56	61.23 ± 27.89	27.55 ± 22.32
NL216	0.79 ± 0.34	0.592 ± 0.44	21.40 ± 11.99	7.00 ± 0.97	51.98 ± 27.78
NL145	0.49 ± 0.69	0.47 ± 0.54	4.67 ± 6.27	12.40 ± 8.34	30.90 ± 9.62

Figure 4. Re-expression of LKB1-KD increases PD-L1 expression. A, Sample flow cytometry data for each murine cell line, demonstrating low levels of PD-L1 expression in all of the parental, *Lkb1*-null lines (vehicle) and high PD-L1 expression in all LKB1-KD lines. Percentage of PD-L1 positive cells is indicated in the bottom right corner of each graph. **B**, Chart illustrating the average percentage of PD-L1-positive cells for each cell line, with standard deviations. Results were quantified using IDEAS software, with gates set so that isotype controls had ≤1% of cells marked positive. Five replicates were conducted in the NL212 and NL216 cell lines; 3 replicates were conducted in the NL145 cell line.

was introduced; in the NL145 line, average PD-L1 expression increased 7.7%. In contrast, when LKB1 was restored in the NL216 line, PD-L1 expression decreased by 14.4%. Across all lines, PD-L1 expression increased in LKB1-KD mutants (24.0% in NL212, 30.6% in NL216, and 26.23% in NL145). It is currently unclear why the loss of LKB1 kinase function but not total loss of LKB1 results in high PD-L1 levels. Further characterization of LKB1's kinase activity is necessary. However, these results demonstrate that a relationship between LKB1 status and PD-L1 expression may indeed exist, indicating that *LKB1* has potential to serve as a biomarker for response to immune checkpoint inhibitor therapies.

UV-exposed *TpLNR* mice develop melanoma more slowly than *TpNR* mice

To confirm that LKB1 loss promotes metastasis both *in vitro* and *in vivo*, *TpLNR* mice, containing conditional knock-in (i.e. *LSL-N-Ras*^{Q61R} and *Rosa26-YFP*) and knock-out (i.e. *p16*^{L} and *LKB1*^{L}) alleles (Figure 5A), and *TpNR* mice, containing *LSL-N-Ras*^{Q61R}, *Rosa26-YFP*, and *p16*^{L} alleles, were compared following exposure to UV radiation (Figure 5B). With regard to melanoma-free survival, *TpNR* mice developed melanomas first, at a median age of 5 weeks, whereas *TpLNR* mice developed melanomas at a median age of 8.43 weeks (Figure 5C). Upon sacrifice, average tumor burden was significantly higher in the *TpNR* mice (an average of 4.4 tumors/ animal vs. 1.4 tumors/animal in *TpLNR* mice; Figure 5D), however, many of the *TpLNR* mice in the study are still young and have yet to develop melanomas. Tumors in the two cohorts of mice had similar tumor growth rates once established (Figure 5D).

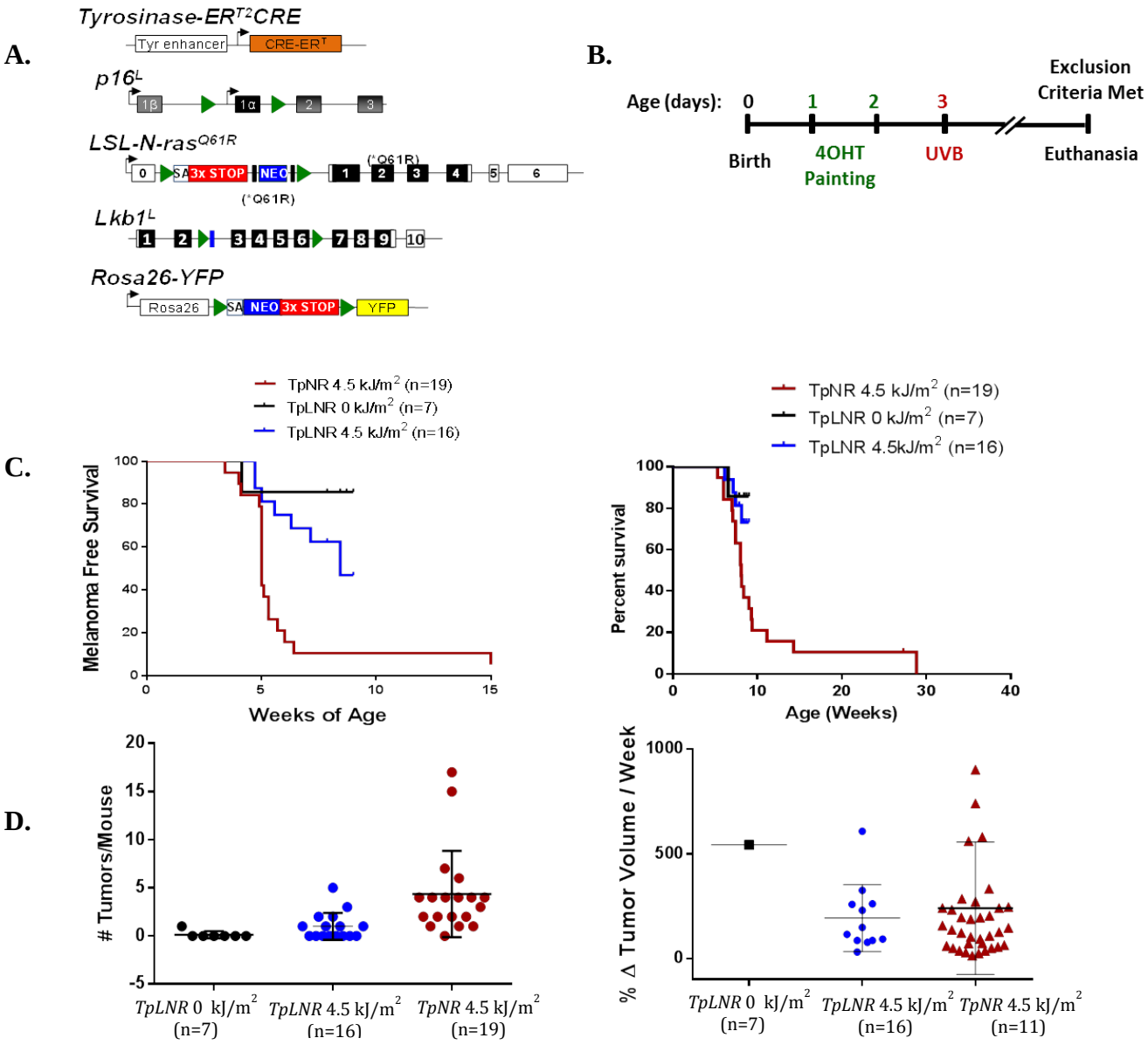

Figure 5. *TpLNR* mice exposed to UV radiation develop tumors more quickly than their non-exposed counterparts, but less quickly than *TpNR* mice. A, Shown are schematics for the alleles used to generated *TpLN*^{Q61R}-YFP lineage tracer mice. All mice in the present study carry the *Tyr-CRE-ER*^{T2} transgene and are homozygous for the *p16*^{L}, *LKB1*^{L}, *LSL-N-rasQ61*, and *Rosa26-YFP* alleles. **B**, Timeline for CRE Recombinase activation and UV exposure. Mice were split into ultra-violet (UV) exposure and non-exposure groups at a 3:1 ratio. **C**, *Left*, Kaplan-Meier curves showing that in *TpLNR* mice, median melanoma-free survival is higher than in *TpNR* mice (8.43 weeks vs. 5 weeks). *Right*, Kaplan-Meier curves showing the overall survival of *TpLNR* and *TpNR* mice. **D**, *Left*, *TpLNR* mice exposed to UV radiation develop more tumors than their non-exposed counterparts, but develop fewer tumors than *TpNR* mice (an average of 1.4 tumors/animal in *TpLNR* mice vs. an average of 4.4 tumors/ animal in *TpNR* mice); however, many of the *TpLNR* mice are still young and have yet to develop melanomas. *Right*, Growth rates of both spontaneous and UV-induced tumors in *TpLNR* mice, as measured by calipers.

UV exposure promotes melanocytic hyperproliferation and macrometastases in *TpLNR* mice

To evaluate the cooperation between *LKB1* and UV radiation in the development of macrometastases, *TpLNR* mice were dissected following UV exposure and melanoma formation. In necropsies, UV-exposed *TpLNR* mice exhibit severe melanocytic hyperproliferation along their tails, ears, and paws, which is not observed in non-exposed counterparts (Figure 6A). UV-exposed mice also show pronounced evidence of macrometastases to the lymph node, spleen, liver, and brain (Figure 6B). These results mimic clinical findings, in which the most common sites of regional melanoma metastasis are lymph nodes and for distant metastasis are the skin, lung, brain, liver, bone, and intestine[20]. In other studies performed by our lab, *TpNR* mice, which maintain functional *LKB1*, have less evidence of macrometastases (<10%), with the most common observations being multiple secondary skin tumors and enlarged, darkened lymph nodes.

A.

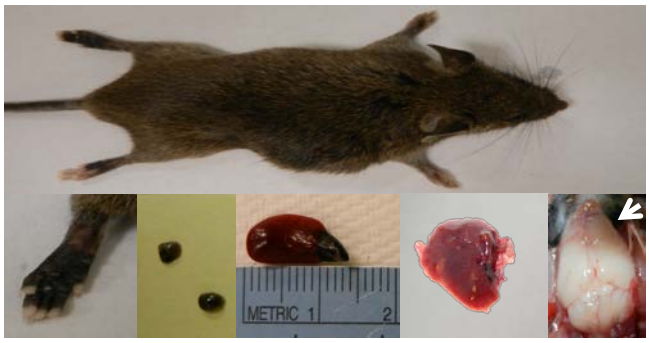

B.

	Lymph Nodes	Spleen	Liver	Lungs	Brain
Frequency of Abnormality	4/4	3/4	2/4	0/4	1/4

Figure 6. *TpLNR* mice exposed to UV radiation show evidence of macrometastases and other melanocytic hyperplasia. A, Shown are typical phenotypes of the UV-exposed *TpLNR* animals. *Top*, An animal that has developed aggressive melanoma on its flank. *Bottom left*, Example of melanocytic hyperproliferation on the paw, believed to be attributable to *Lkb1* loss. *Bottom center and right*, Evidence of metastasis: enlarged, pigmented lymph nodes, pigmented spleen, lesions along one lobe of liver and a lesion on the frontal lobe of the brain. **B**, Chart indicating the number of UV-exposed *TpLNR* mice with putative macrometastases in each organ type.

Discussion

The role of LKB1 in migration

Our work establishes that migration in murine melanoma cell lines is LKB1-dependent, and partially contingent on LKB1's kinase function. However, there was high variability between cell lines with regard to the impact of LKB1 on migration. The three murine melanoma cell lines used in this study came from *TpLN* mice which harbor identical driver mutations (loss of the p16 and LKB1 tumor suppressors as well as a Q61R mutation in the NRAS proto-oncogene); however, it is impossible to know which secondary mutations may have occurred to promote the development of the melanomas. These secondary mutations may play a role in the migratory ability of the cells and influence the impact of LKB1 reintroduction. Further characterization of each cell line will be necessary to understanding why LKB1 differentially alters the migratory potential of each line. Furthermore, as LKB1 plays a role in multiple signaling pathways, it is possible that changes in migratory rates in LKB1-deficient, LKB1-proficient, and LKB1-KD cells are attributable to altered expression of proteins downstream of LKB1, such as AMP-activated protein kinase (AMPK). It will therefore be important to evaluate the impact of LKB1 loss/reintroduction on multiple downstream proteins in each cell line. Finally, to provide further data on each cell line's migratory potential, Boyden chamber migration assays could also be performed, and the results compared to the wound healing assay data.

Drawbacks in the infection methods used may also provide a potential explanation for LKB1's variable impact. The LKB1 and LKB1-KD viruses were not titered and therefore, infection rates in each cell line may differ. Inconsistent viral uptake within each cell line likely resulted in some

cells incorporating multiple copies of LKB1 while others incorporated very few. These inconsistencies could have profound impacts on not only the results of our migration assays, but also on ourflow cytometry findings. To ensure consistency in LKB1 expression for future experiments, it would be important to titer the virus prior to infection and to then form clonal populations within each cell line. To further assure similar LKB1 expression between cell lines, RT-PCR for *LKB1* mRNA could be performed.

Potential for *LKB1* as a biomarker for checkpoint inhibitor therapies

Our flow cytometry results reveal a potential relationship between LKB1 expression and PD-L1. Should these results prove true in future trials, this would lend support to the idea that patients with tumors harboring *LKB1* deletions are not suitable candidates for immune checkpoint inhibitor therapies targeting the PD-1-PD-L1 interaction, unless LKB1 expression could be restored. These results differ from the previously mentioned lung cancer studies by Xu *et al*., where it was found that loss of *LKB1* correlated with high PD-L1 levels[14]. This difference may be attributable to the multitude of pathways that regulate PD-L1 and the differing importance of each pathway in lung cancer versus melanoma. For example, one such pathway is the PI3K/Akt-mTOR pathway, in which LKB1 is thought to inhibit the phosphorylation of mTOR, causing a downstream reduction in PD-L1 expression. Xu *et al.* found that this pathway in particular was heavily implicated in lung cancer[14]; in melanoma, however, the Ras-MAPK pathway, which also regulates PD-L1 expression, is more relevant[16] and may play a larger role in regulating PD-L1 expression, which could explain why the presence of LKB1 did not eliminate PD-L1 expression. Future mechanistic studies are needed to determine why *LKB1-KD* is sufficient to restore PD-L1 expression. Our next step in elucidating LKB1-KD's relationship with PD-L1 will

be to perform a co-immunoprecipitation to determine what exactly LKB1-KD is binding. As revealed by the standard deviations present in Figure 4B, there is high variability even between trials in each cell line. Optimization of protocols may be important moving forward, and it will also be crucial to complete more trials to gain reliable results. As mentioned earlier, greater consistency may be achieved by creating clonal populations to account for the amount of *LKB1* present in each cell line. Additionally, the relationship between *LKB1* and PD-L1 *in vivo* should be examined by immunohistochemistry (IHC) in tumor samples from both the *TpLNR* (lacking LKB1) and *TpNR* models (containing functional LKB1).

The TpLNR-UV mouse model as a genetically faithful model of human melanoma

Though several metastatic melanoma mouse models exist today, many lack clinical relevance. As previously mentioned, some utilize RAS isoforms that are rarely observed in human melanomas[16], while others overexpress NRAS at super-physiological concentrations[17], reducing the ability to generalize results to human patients. The present study, however, has established a clinically-relevant, UV-induced *NRAS*-driven melanoma mouse model that allows for characterization of the role of *LKB1* in metastasis *in vivo*. This model can be used to better establish the organs to which *LKB1*-null, *NRAS*-mutant melanomas metastasize and quantify the frequency of these metastases. Ultimately, this model will be invaluable for understanding metastases in melanoma and could provide a way to test future therapeutics.

A major drawback to this mouse line is the inability to characterize micrometastases. Though analysis of organs during necropsy has made it is possible to observe large-scale metastatic lesions, it is highly likely that smaller micrometastases are occurring and go unnoticed. The

Rosa26-LSL-YFP allele incorporated in these mice, meant to enable visualization of melanocytes throughout the body, has proven unsuccessful. While genotyping has confirmed that the allele is present in the mice, recent YFP staining and fluorescent microscopy of tissue samples has been incapable of detecting any YFP. At this time, we are uncertain whether the problem lies in the gene's recombination, a problem with its insertion point, or something different altogether; therefore, this allele is currently insufficient in tracking melanocytes throughout the bodies of our mice. To ascertain whether there may be a problem in transcription of the gene, future experiments include evaluating YFP mRNA levels by performing RT-PCR on tumor samples; similarly, we will lyse tumor samples and perform an immunoblot for YFP to determine whether any YFP protein is present. Due the barriers we have met with this allele, we are presently working to introduce a different lineage tracer, Rosa26-LSL-LacZ, into our *TpLN* mice to provide more reliable detection of melanocyte-derived malignancies. Future studies with these mice will allow for more sensitive characterization of *LKB1*-related metastases in *NRAS*-driven melanomas.

Acknowledgments

I would like to thank the following individuals for their assistance throughout the course of this study: Rebecca C. Hennessey, Xiangnan Guan, Andrea Holderbaum, Meriam Waqas, and Dr. Christin E. Burd. I would also like to thank the Lesinski and Guttridge labs at the Ohio State University for their assistance with the PD-L1 flow cytometry portion of my project.

This work was supported by a Pelotonia Undergraduate Fellowship (to R.M.U.).

References

1. Society, A.C., *Cancer Facts and Figures 2016,* 2016: Atlanta. p. 4-21.
2. Bhatia, S., S.S. Tykodi, and J.A. Thompson, *Treatment of metastatic melanoma: an overview.* Oncology 2009. **23**(6): p. 488-96.
3. Chapman, P.B., et al., *Phase III multicenter randomized trial of the Dartmouth regimen versus dacarbazine in patients with metastatic melanoma.* J Clin Oncol, 1999. **17**(9): p. 2745-51.
4. Atkins, M.B., et al., *High-dose recombinant interleukin 2 therapy for patients with metastatic melanoma: analysis of 270 patients treated between 1985 and 1993.* J Clin Oncol, 1999. **17**(7): p. 2105-16.
5. Lev, D.C., et al., *Exposure of melanoma cells to dacarbazine results in enhanced tumor growth and metastasis in vivo.* J Clin Oncol, 2004. **22**(11): p. 2092-100.
6. Alliance, M.R., *Raising the Bar: Accelerating New Paradigms in Melanoma Research,* 2015: Washington D.C. p. 4-8.
7. Guha, M., *Immune checkpoint inhibitors bring new hope to cancer patients.* The Pharmaceutical Journal, 2014. **293**.
8. Kim, T., et al., *Combining targeted therapy and immune checkpoint inhibitors in the treatment of metastatic melanoma.* Cancer Biol Med, 2014. **11**(4): p. 237-46.
9. Sanchez-Cespedes, M., et al., *Inactivation of LKB1/STK11 Is a Common Event in Adenocarcinomas of the Lung.* Cancer Research, 2002. **62**(3659).
10. Zhuang, Z.G., et al., *Enhanced expression of LKB1 in breast cancer cells attenuates angiogenesis, invasion, and metastatic potential.* Mol Cancer Res, 2006. **4**(11): p. 843-9.

11. Guldberg, P., et al., *Somatic mutation of the Peutz-Jeghers syndrome gene, LKB1/STK11, in malignant melanoma.* Oncogene, 1999. **18**(9): p. 1777-80.

12. Liu, W., et al., *LKB1/STK11 inactivation leads to expansion of a prometastatic tumor subpopulation in melanoma.* Cancer Cell, 2012. **21**(6): p. 751-64.

13. Forbes, S.A., et al., *COSMIC: exploring the world's knowledge of somatic mutations in human cancer.* Nucleic Acids Res, 2015. **43**(Database issue): p. D805-11.

14. Xu, C., et al., *Loss of Lkb1 and Pten leads to lung squamous cell carcinoma with elevated PD-L1 expression.* Cancer Cell, 2014. **25**(5): p. 590-604.

15. Lee M.H., et al., *Increased PD-L1 expression in KRAS mutated premalignant human bronchial epithelial cells is enhanced by LKB1 loss and mediated by ERK activation.* Journal for ImmunoTherapy of Cancer, 2015. **3**.

16. Burd, C.E., et al., *Mutation-specific RAS oncogenicity explains NRAS codon 61 selection in melanoma.* Cancer Discov, 2014. **4**(12): p. 1418-29.

17. Haigis, K.M., et al., *Differential effects of oncogenic K-Ras and N-Ras on proliferation, differentiation and tumor progression in the colon.* Nat Genet, 2008. **40**(5): p. 600-8.

18. Trimboli, A., et al., *Pten in Stromal Fibroblasts Suppresses Mammary Epithelial Tumors.* Nature, 2009. **461**(7267): p. 1084-1091.

19. Monahan, K.B., et al., *Somatic p16(INK4a) loss accelerates melanomagenesis.* Oncogene, 2010. **29**(43): p. 5809-17.

20. Damsky, W.E., L.E. Rosenbaum, and M. Bosenberg, *Decoding melanoma metastasis.* Cancers (Basel), 2010. **3**(1): p. 126-63.